

# Smart Ionic Sol–Gel-Based Azobenzene Materials for Optical Generation of Microstructures

Olga Kulikovska,<sup>†</sup> Leonid M. Goldenberg,<sup>‡</sup> Lazar Kulikovsky,<sup>‡</sup> and Joachim Stumpe<sup>\*,†,‡</sup>

Fraunhofer Institute for Applied Polymer Research, Science Campus Golm, Geiselbergstr. 69, 14476 Potsdam, Germany, and Institute of Thin Film Technology and Microsensorics, Kantstr. 55, 14513 Teltow, Germany

Received January 10, 2008. Revised Manuscript Received February 19, 2008

We propose a concept of supramolecular materials for effective all-optical generation of surface relief structures. The materials are based on the ionic interactions between oppositely charged photochromic azobenzene units and polysiloxane backbones formed in situ. The materials are easy to produce from commercial components. Using ionic interactions to connect photochromic units to the polymer backbones allowed very high dye-doping levels without aggregation. Because of this noncovalent bonding the polymer chains got involved in the photoinduced translation motion of azobenzene units resulting in very effective formation of surface relief gratings. For the first time some relaxation processes which counteract the light-induced formation of surface relief structures were suggested. Under consideration of these processes the influence of network formation and alternatively of glassy state on the efficiency of mass transport and the stability of induced structures was discussed. Because of the simplicity and versatility of the concept the new family of materials for applications in optics, sensorics, and biology may be designed.

## 1. Introduction

Azobenzene-containing materials have been well-known for the induction of dichroism and birefringence upon irradiation with polarized light. The mechanism involves repeating *E–Z* photoisomerization and relaxation of azobenzene chromophores resulting in the orientation of azobenzene units perpendicularly to the polarization of the irradiating light. Both stable and dynamic anisotropy has been induced, and birefringence gratings have been inscribed in a variety of materials.<sup>1–8</sup> Later on the formation of surface relief gratings (SRG) has been observed in films of the azobenzene functionalized polymers under holographic exposure.<sup>9,10</sup> Since then the formation of SRG has been demonstrated in a variety of the azobenzene-containing materials in-

cluding dye-doped systems,<sup>11</sup> functionalized polymers,<sup>12,13</sup> Langmuir–Blodgett and layer-by-layer films,<sup>14</sup> film forming low molecular weight materials,<sup>15–17</sup> hybrid sol–gel matrices,<sup>18–20</sup> and materials based on the ionic and hydrogen-bonding interactions.<sup>21–23</sup> The SRGs, all optically formed in the thin films, show very high diffraction efficiencies, near the theoretical limit for Raman–Nath diffraction regime, and therefore are very prospective for

\* To whom correspondence should be addressed. Phone: +49 331 568 1259. Fax: +49 331 568 3259. E-mail: stumpe@iap.fhg.de.

<sup>†</sup> Fraunhofer Institute for Applied Polymer Research.

<sup>‡</sup> Institute of Thin Film Technology and Microsensorics.

- (1) Rochon, P.; Gosselin, G.; Natansohn, A.; Xie, S. *Appl. Phys. Lett.* **1992**, *60*, 4.
- (2) Lagugné-Labarthe, F.; Buffeteau, T.; Sourisseau, C. *J. Phys. Chem. B* **1998**, *102*, 2654.
- (3) Zucolotto, V.; Strack, P. J.; Santos, F. R.; Balogh, D. T.; Constantino, C. J. L.; Mendonca, C. R.; Oliveira, O. N. *Thin Solid Films* **2004**, *453–454*, 110.
- (4) Silva, J. R.; Dall'Agnol, F. F.; de Souza, N. C.; Oliveira, O. N., Jr.; Giacometti, J. A. *Synth. Met.* **2003**, *138*, 153.
- (5) Ilieva, D.; Li, N.; Petrova, T.; Tomova, N.; Dragostinova, V.; Nikolova, L. *J. Optics A* **2005**, *7*, 35.
- (6) Fukuda, T.; Kim, J. Y.; Barada, D.; Yase, K. *Proc. SPIE* **2006**, *6136*, 61360Y.
- (7) Ramanujam, P. S.; Dam-Hansen, C.; Berg, R. H.; Hvilsted, S.; Nikolova, L. *Optics Lasers Eng.* **2006**, *44*, 912.
- (8) Ke, X.; Yan, X.; Song, S.; Li, D.; Yang, J. J.; Wang, M. R. *Opt. Mater.* **2007**, *29*, 1375.
- (9) Rochon, P.; Batalla, E.; Natansohn, A. *Appl. Phys. Lett.* **1995**, *66*, 136.
- (10) Kim, D. Y.; Tripathy, S. K.; Li, L.; Kumar, J. *Appl. Phys. Lett.* **1995**, *66*, 1166.

- (11) Fiorini, C.; Prudhomme, N.; de Veyrac, G.; Maurin, I.; Raimond, P.; Nunzi, J.-M. *Synth. Met.* **2000**, *115*, 121.
- (12) Natansohn, A.; Rochon, P. *Chem. Rev.* **2002**, *102*, 4139.
- (13) Viswanathan, N. K.; Kim, D. Y.; Bian, S.; Williams, J.; Liu, W.; Li, L.; Samuelson, L.; Kumar, J.; Tripathy, S. K. *J. Mater. Chem.* **1999**, *9*, 1941.
- (14) (a) He, J.-A.; Bian, S.; Li, L.; Kumar, J.; Tripathy, S. K.; Samuelson, L. A. *J. Phys. Chem. B* **2000**, *104*, 10513. (b) Oliveira, J.; Osvaldo, N.; dos Santos, J.; David, S.; Balogh, D. T.; Zucolotto, V.; Mendonca, C. R. *Adv. Coll. Inter. Sci. A* **2005**, *116*, 179.
- (15) Ishow, E.; Lebon, B.; He, Y.; Wang, X.; Bouteiller, L.; Galmiche, L.; Nakatani, K. *Chem. Mater.* **2006**, *18*, 1261.
- (16) Perschke, A.; Fuhrmann, T. *Adv. Mater.* **2002**, *14*, 841.
- (17) Nakano, H.; Takahashi, T.; Kadota, T.; Shirota, Y. *Adv. Mater.* **2002**, *14*, 1157.
- (18) Darracq, B.; Chaput, F.; Lahlil, K.; Lévy, Y.; Boilot, J.-P. *Adv. Mater.* **1998**, *10*, 1133.
- (19) del Monte, F.; Ramos, G.; Belenguer, T.; Levy, D. *Proc. SPIE* **2002**, *4802*, 51.
- (20) Boilot, J. P.; Biteau, J.; Chaput, F.; Gacoin, T.; Brun, A.; Darracq, B.; Georges, P.; Levy, Y. *Pure Appl. Optics* **1998**, *7*, 169.
- (21) Kulikovska, O.; Goldenberg, L. M.; Stumpe, J. *Chem. Mater.* **2007**, *19*, 3343.
- (22) Goldenberg, L. M.; Kulikovska, O.; Stumpe, J. *Langmuir* **2005**, *21*, 4794.
- (23) (a) Gao, J.; He, Y.; Liu, F.; Zhang, X.; Wang, Z.; Wang, X. *Chem. Mater.* **2007**, *19*, 14–3877.
- (24) Natansohn, A.; Rochon, P. *Adv. Mater.* **1999**, *11*, 1387.
- (25) Baac, H.; Lee, J.-H.; Seo, J.-M.; Park, T. H.; Chung, H.; Lee, S.-D.; Kim, S. J. *J. Mater. Sci. Eng., C* **2004**, *24*, 209.
- (26) Ye, C.; Wong, K. Y.; He, Y.; Wang, X. *Opt. Expr.* **2007**, *15*, 936.
- (27) Kim, J. Y.; Kim, T. H.; Kimura, T.; Fukuda, T.; Matsuda, H. *Opt. Mater.* **2002**, *21*, 627.

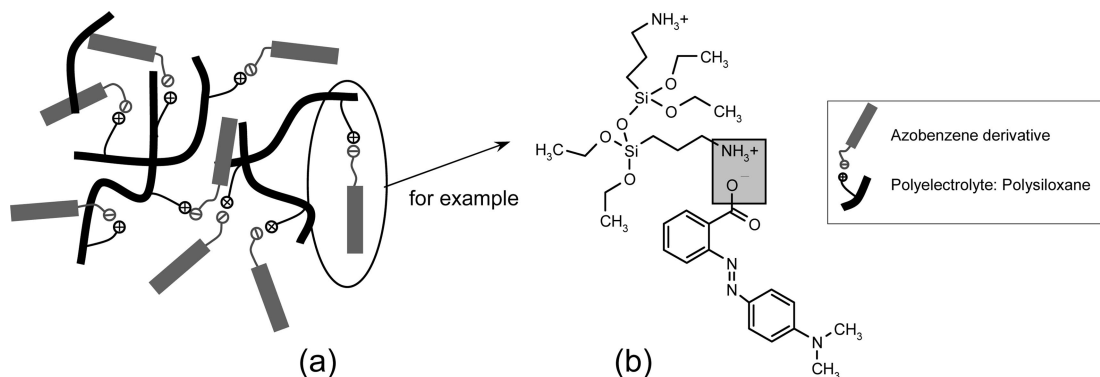


**Figure 1.** Schematic presentation of an azobenzene-based supramolecular sol–gel material with ionic interactions (a); an example of complex formation (b).

many applications in optics and information technologies.<sup>13,14,24–27</sup>

The process of the SRG formation implies the translational motion of the azobenzene chromophores on the scale of micrometers. The light-induced motion of the photochromic units eventually involves polymer backbones resulting in microscopic mass transport. In fact this has restricted the choice of the azobenzene materials capable of the effective mass transport to the systems with the azobenzene units covalently attached to the polymer backbone. The effective formation of SRG has been reported mostly in the azobenzene functionalized systems including polymers<sup>12,13</sup> and hybrid films prepared by the sol–gel technique using azobenzene functionalized siloxane precursors.<sup>18</sup> A big drawback of such systems is the multistep synthesis required for each combination of polymer and chromophore that makes them rather expensive for applications. We have demonstrated an effective induction of optical anisotropy and SRG in azobenzene functionalized polyelectrolyte system PAZO.<sup>22</sup> The PAZO-based SRGs were quite effective and extremely thermally stable. In our recent work<sup>21,28</sup> we have shown for the first time the effective formation of SRG in the supramolecular complexes of oppositely charged azobenzene derivatives and polyelectrolytes, i.e. in the systems where the chromophores are attached to the passive polyelectrolyte chains by noncovalent interactions. Self-organizing supramolecular structures originating from the complexation of polyelectrolytes with ionic species are promising for the development of smart materials.<sup>29</sup> One could expect these complexes to have the optical response of the azobenzenes; namely, they exhibit the nonlinear optical properties,<sup>30</sup> *E–Z* isomerization, and orientation.<sup>21</sup> The new and unexpected phenomenon that we have demonstrated was the fact that the passive polyelectrolyte chains connected only by ionic interactions to the azobenzene moieties got involved in their light-induced translational motion. We have proven that, alternatively to the covalent bonding, the noncovalent interactions provide for the photoinduced mass transport.<sup>21,28</sup>

SRGs with the surface modulation depth up to 1.65  $\mu\text{m}$  have been obtained using these materials. Moreover, due to ionic nature of these supramolecular materials the thermal stability of inscribed SRG is higher than in many azobenzene-functionalized materials reported up to now. However, caused by the hydroscopic nature of polyelectrolytes the films are prone to the influence of surrounding. We apply here the developed supramolecular approach to the polyelectrolyte formed in situ by the sol–gel reaction of alkoxy silane (Figure 1).<sup>28</sup> We demonstrate the effective formation of SRG combined with high thermal and long-time stability in the azobenzene containing materials of this new type. The materials with targeted properties may be easily formulated from readily available and nonexpensive commercial components. This supramolecular approach opens wide possibilities for simple, cost-effective and environment friendly preparation of a variety of materials for the effective formation of SRG from building blocks.

## 2. Experimental Section

**Materials.** Chemical formulas of compounds are displayed in Figure 2.

Brilliant Yellow A (80 mg, 0.09 mmol) (Aldrich, 70%) in 2 mL of MeOH was mixed with 130 mg (0.59 mmol) of (3-aminopropyl)triethoxysilane S (APTES, Witco Europa SA). After the addition of 10  $\mu\text{L}$  of concentrated HCl, the solution was left to settle, clear red mother solution decanted, and used for film preparation. Also higher concentrations of Brilliant Yellow (up to A:S = 1:1) were used.

5-(4-Aminophenylazo)salicylic acid sodium salt (38 mg) B (Aldrich, 30%) in 1 mL of MeOH was mixed with 180 mg of S. After addition of 10  $\mu\text{L}$  of concentrated HCl, the solution was left to settle, clear red mother solution decanted, and used for film preparation.

2-(4-Dimethylaminophenylazo)benzoic acid, Na salt C (90 mg, 0.31 mmol, Aldrich), in 2 mL of MeOH was mixed with 70  $\mu\text{L}$  (0.3 mmol) of S. After the addition of 20  $\mu\text{L}$  (0.3 mmol) of concentrated HCl, the solution was left to settle, clear red mother solution decanted, filtrated through a 0.2- $\mu\text{m}$  Nalgene filter, and used for the film preparation.

2-(4-Dimethylaminophenylazo)benzoic acid D (210 mg, 0.78 mmol) in 1 mL of MeOH (not soluble) was solubilized upon addition of 180  $\mu\text{L}$  (0.78 mmol) of S. After filtration the solution was used for the film preparation.

4-(4-Dimethylaminophenylazo)benzoic acid E (312 mg, 1.16 mmol, Aldrich) in 35 mL of MeOH was mixed with 270  $\mu\text{L}$  (1.16

(28) Stumpe, J.; Goldenberg, L.; Kulikovska, O. PCT Patent Application WO2006/024500.

(29) (a) Thünemann, A. F.; Schnöller, U.; Nuyken, O.; Voit, B. *Macromolecules* **2000**, *33*, 5665. (b) Thünemann, A. F. *Prog. Polym. Sci.* **2002**, *27*, 1473.

(30) (a) Meyer, W. H.; Pecherz, J.; Mathy, A.; Wegner, G. *Adv. Mater.* **1991**, *3*, 153. (b) Priimagi, A.; Cattaneo, S.; Ras, R. H. A.; Valkama, S.; Ikkala, O.; Kauranen, M. *Chem. Mater.* **2005**, *17*, 5798.

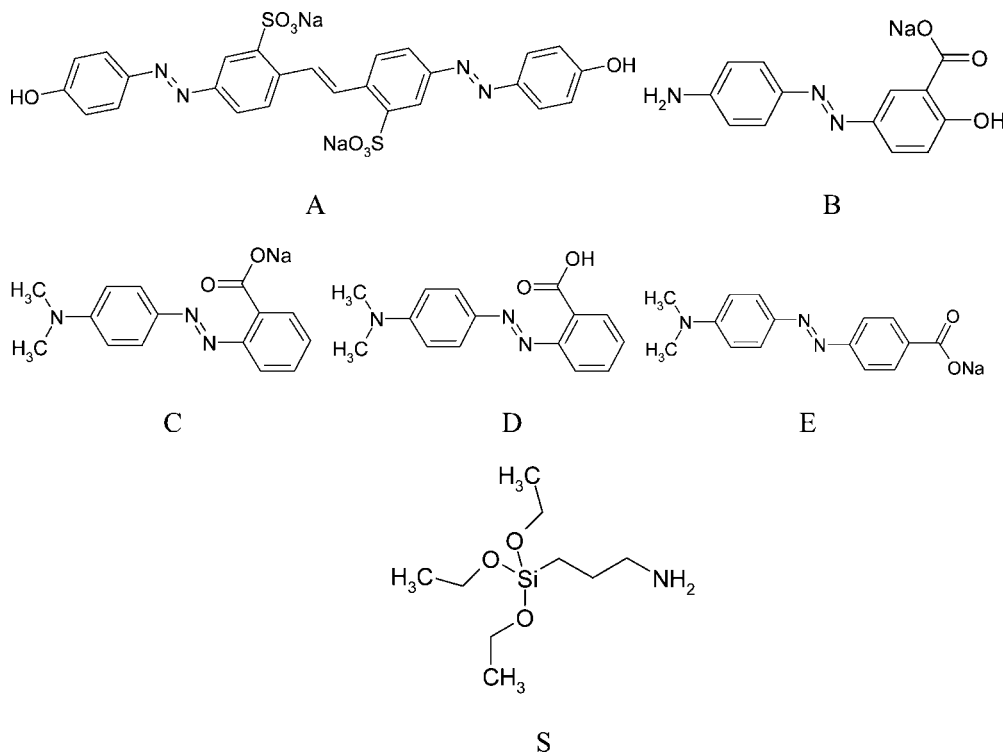


**Figure 2.** Examples of compounds used for materials preparation: (A–E) azobenzene derivatives; (S) alkoxy silane.

mmol) of S. After addition of 10  $\mu\text{L}$  (1.16 mmol) of concentrated HCl the solution was left to settle, clear red mother solution decanted, filtrated through a 0.2- $\mu\text{m}$  Nalgene filter, reduced in volume about twice by evaporation, and used for the film preparation.

The films of 0.5–2- $\mu\text{m}$  thickness were prepared from above-described solutions by casting, doctor-blading, or spin-coating.

**Measurements.** FTIR spectra were measured by Mattson Instruments RS 10000 FTIR spectrometer using the film cast onto Si substrates, and UV–vis spectra were measured by a Perkin-Elmer Lambda 2 spectrometer. Differential scanning calorimetry (DSC) was measured by Netzsch DSC 204 in  $\text{N}_2$  atm.

For SRG inscription the films were irradiated with the interference pattern of two orthogonally polarized beams from an  $\text{Ar}^+$  ion laser operating at the wavelength of 488 nm. The beams were polarized linearly with polarization planes at  $\pm 45^\circ$  to the incidence plane unless otherwise noted. An angle between two interfering beams was about  $17^\circ$  resulting in a period of 1.65  $\mu\text{m}$ . The intensities of irradiating beams were equal to 250  $\text{mW}/\text{cm}^2$ . The grating formation was probed by diffraction of a weak probe beam from a He–Ne laser. The intensities of zeroth-,  $\pm$ first-, and  $\pm$ second-diffraction orders were measured during grating recording. The surface relief gratings were then verified by atomic force microscopy (AFM) performed at Solver P47H Smena (NTMDT) in semicontact mode.

### 3. Results and Discussion

Although sol–gel materials based on polysiloxane have been known for their durability, so far the only examples of sol–gel-based materials for SRG inscription are materials synthesized from alkoxy silane bearing azobenzene and carbazole moieties.<sup>18,31,32</sup> The sol–gel azobenzene materi-

als based on 3-(triethoxysilyl)propyl isocyanate though being thermally stable up to the glass transition temperature (150–160  $^\circ\text{C}$ ) are capable of only noneffective light-induced mass transport.<sup>33</sup> While the covalent bonding of azobenzene to the matrix was considered to favor the stability of the induced birefringence,<sup>20,34</sup> the cross-linking of the sol–gel materials has been reported as hindrance for SRG formation.<sup>18,31</sup>

In this study we report new materials with azobenzene chromophores attached to the ionic matrix by noncovalent interactions, whereas the matrix is formed in situ by a sol–gel reaction of alkoxy silane (Figure 1). The cross-linking process was optimized to get effective light-induced mass transport in combination with a long shelf life and high thermal stability of induced relief structures. As active components we used commercially available ionic azobenzene derivatives shown in Figure 2 (compounds A–E). The aminosubstituted alkoxy silane APTES (compound S in Figure 2) was used as passive component. The materials were produced by mixing of alcoholic solutions of the azobenzene derivatives, and compound S followed by sol–gel reaction catalyzed by HCl.

The most effective SRGs were formed in the materials containing the azobenzene derivatives C and D, with diffraction efficiencies up to 45%. The formulations with compounds A and B exhibited less effective grating formation with diffraction efficiencies up to 8%. No reasonably good films were obtained from the formulation with compound E, and the inscribed gratings were not appreciable,

(31) Chaput, F.; Lahlil, K.; Biteau, J.; Boilot, J.-P.; Darracq, B.; Levy, Y.; Peretti, J.; Safarov, V. I.; Lehn, J.-M.; Fernandez-Acebes, A. *Proc. SPIE* **2000**, 3943, 32.

(32) Frey, L.; Darracq, B.; Chaput, F.; Lahlil, K.; Jonathan, J. M.; Roosen, G.; Boilot, J. P.; Levy, Y. *Opt. Commun.* **2000**, 173, 11.

(33) Kim, M.-R.; Choi, Y.-I.; Park, S.-W.; Lee, J.-W.; Lee, J.-K. *J. Appl. Polym. Sci.* **2006**, 100, 4811.

(34) Marino, I. G.; Bersani, D.; Lottici, P. P. *Opt. Mater.* **2000**, 15, 175.

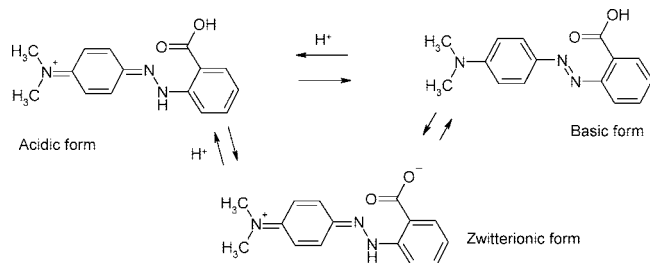


**Figure 3.** Forms of the azobenzene compound D.

although the azobenzene E differs from C only by the position of the carboxyl substituent. Further investigations were concentrated on the most effective materials with azobenzene derivatives C and D.

According to Ramette et al.,<sup>35</sup> azobenzene derivative D exists in three forms shown in Figure 3, including the yellow basic form, the intensively red protonated acidic form, and the intermediate zwitterionic form with absorption maxima at 406, 521, and 491 nm in MeOH, respectively.<sup>36</sup> However, only the basic form that can undergo *E–Z* photoisomerization is germane to the light-induced mass transport. Correspondingly, the amino groups of matrix compound S have to be protonated to create positively charged species as counterions for negatively charged carboxylate anions of C as it is shown in Figure 1. We used for this HCl in stoichiometric ratio to S. Exceeding the ratio of HCl could shift the dye into the quinoid form (Figure 3) where the *E–Z* isomerization is effectively suppressed. As expected, no SRG could be written in these films. On the basis of estimated  $pK_a$  values,<sup>37</sup> it may be suggested that by the addition of 1 equiv of HCl that the amino group of S will be protonated. The protonated amino group can then interact with azobenzene anion leading to the complex formation.

Similar consideration may be applied to the azobenzene dye in form D. In this case proton transfer from the carboxylic group of D to the amino group of S takes place. It benefits the solubility of the azobenzene compound D. The absorption maximum in the UV–vis spectrum and the absence of the COOH vibration band in FTIR spectrum<sup>38</sup> of the film similar to that in ref 21 prove the yellow basic form (Figure 3) of the azobenzene dye D in the film and thus further on confirm the concept of supramolecular complex formation.

The described above noncovalent bonding of azobenzene units to the matrix is essential for light-induced mass transport. First, it allows higher loading of azobenzene chromophores without aggregation. Typically dye aggregation has limited its loading in the guest–host systems to 10 and 30% for specially synthesized dyes with higher solubility in polymer matrix.<sup>11</sup> In the presence of strong noncovalent interactions the aggregation is suppressed allowing loading level, which typically has been achieved only by covalent

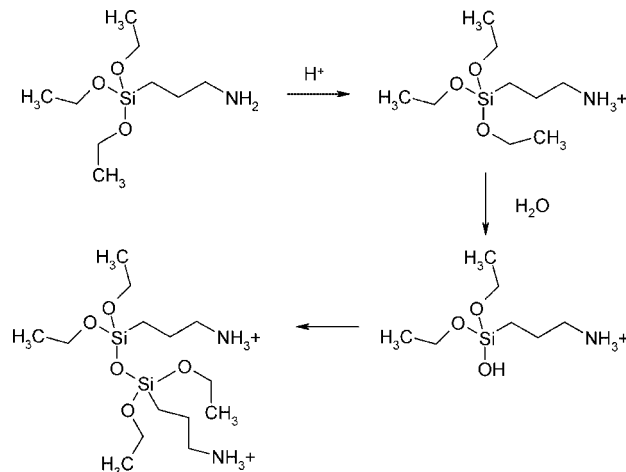


**Figure 4.** Scheme of condensation reactions of the compound S.

bonding of the dye molecules to the polymer.<sup>30</sup> In this study dye concentrations of higher than 55% were readily achieved. Second, noncovalent bonding involves the passive polymer backbone into the translational motion of chromophores. The latter is only possible if polymer chains are still flexible enough to move. In the case of sol–gel materials, the degree of freedom of the polymer backbone is determined by the extent of cross-linking.

Possible reactions of compound S shortened to the first step of condensation are shown in Figure 4. The degree of condensation and the degree of cross linking could be tuned by the choice and amount of catalyst and the choice of the solvent. It is known that in absolute alcohol the condensation reaction is rather slow.<sup>39,40</sup> In this study these effects were used to avoid network formation which will inevitably lead to the restriction of the mass transport. The prepared solutions were stable for a long time and could be used any time to prepare photoactive films.

The solutions were readily processed into films by conventional film-building techniques (spin-coating, doctor-blading, casting, spraying, etc.), whereas the best film quality was obtained by spin-coating. After preparation the films were dried at 70 °C for 2–30 min. Such temperature was found to be optimal. It correlates with results of DSC, where presumably polycondensation reaction (weak exothermic peak) is observed at the temperature of about 120 °C during the first heating. Further endothermic peak (at 180 °C) may be ascribed to hidden solvent evaporation. No glass transition has been observed for the investigated materials. This evidences their ionic nature, and we can expect high thermal stability of SRG.

Gratings were recorded using a holographic setup described elsewhere.<sup>41</sup> The samples were irradiated with an interference pattern of two coherent beams at a wavelength of 488 nm within the absorption band of the materials. The orthogonal polarizations of writing beams at  $\pm 45^\circ$  to the incidence plane were used if other is not specified. The period was set to 1.65  $\mu\text{m}$ ; the writing beams intensities were rather

(35) Ramette, R. W.; Dratz, E. A.; Kelly, P. W. *J. Phys. Chem.* **1962**, *66*, 527.

(36) Livingston, R.; Pariser, R. *J. Am. Chem. Soc.* **1948**, *70*, 1510.

(37) Clayden, J.; Geeves, N.; Warren, S. *Organic Chemistry*; Verlag Oxford University Press, 2000.

(38) Silverstein, R. M.; Bassler, G. C.; Morrill, T. C. *Spectrometric Identification of Organic Compounds*; Wiley: New York, 1981.

(39) Piana, K.; Schubert, U. *Chem. Mater.* **1995**, *7*, 1932.

(40) Schubert, U.; Huesing, N.; Lorenz, A. *Chem. Mater.* **1995**, *7*, 2010.

(41) Kulikovska, O.; Gharagozloo-Hubmann, K.; Stumpe, J. *Proc. SPIE* **2002**, *4802*, 85.

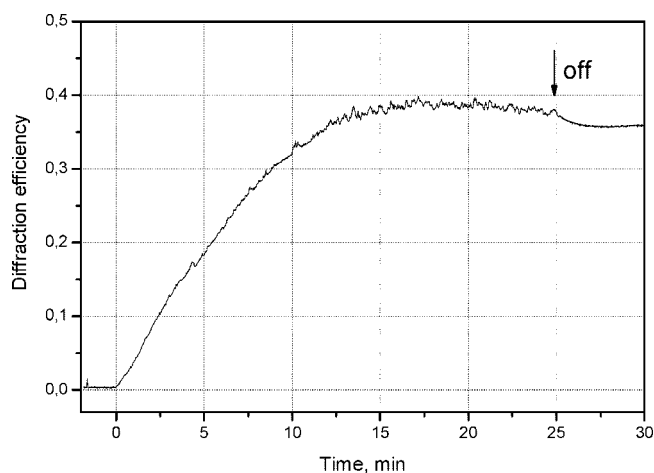


**Figure 5.** Diffraction efficiency of the first diffracted order as functions of recording time. The SRG was recorded in a film of the material C–S.

moderate, and the irradiation times were varied from a few minutes up to one hour. The formation of gratings was probed by linearly horizontally polarized beam at 633 nm, where the absorption of films is low and the low power probe light does not influence the gratings. The diffraction efficiency of  $n$ th-diffracted order was calculated as  $\eta_n = I_n / \Sigma I_n$ , where  $I_n$  are the intensities of the  $n$ th-order diffracted beams. Total diffraction efficiency was determined as the sum of diffraction efficiencies of all nonzero orders  $\eta_{\text{tot}} = \eta_{\pm 1} + \eta_{\pm 2} + \dots$ . Characterizing the recorded gratings by their total diffraction efficiencies proved an advantage especially in the case of deep surface gratings having many diffraction orders in Raman–Nath regime of diffraction. An example of the recording kinetics is shown in Figure 5. Under above experimental conditions, five diffracted orders were observed. The first-order diffraction efficiency of 39% was reached after 17 min of recording in a film of the material C–S. 90% of the probe light ( $\eta_{\text{tot}}$ ) was diffracted by the recorded grating after 20 min. Such high diffraction efficiency can be explained only by high modulation depth of recorded relief grating. Indeed, a grating height of ca. 550 nm was confirmed by AFM measurements. The surface topology and the cross section of the grating are shown in Figure 6. The period of the grating was measured to be 1.65  $\mu\text{m}$  in accordance with the period of the interference pattern. Notice that the profile form deviates from the sinusoidal one that can be explained in terms of the overwriting the grating by the self-diffracted beams. In this case the gratings with smaller modulation depth are expected to have perfectly sinusoidal profiles. It is shown in Figure 7, where the profile of a grating with modulation depth of 175 nm is compared to the sine function. The modulation depths of the recorded gratings were controlled through the irradiation time. After the recording beams were switched off the gratings remain stable as demonstrated in Figure 8. By use of longer inscription times, the gratings with modulation amplitude of higher than 1  $\mu\text{m}$  were written in material C–S.

The efficiencies of gratings formation were investigated for different polarization configurations of the recording beams: linear orthogonal at  $\pm 45^\circ$  to the incidence plane, linear p–p and linear s–s polarizations. The most efficient grating formation was observed in the case of the polarization

recording, i.e. for the linearly orthogonally polarized recording beams. In this case no intensity modulation exists but the light changes the direction and ellipticity of the polarization within the period of the interference pattern. This polarization dependence allows excluding any thermal recording mechanism. For example, the total diffraction efficiencies of 58 and 27% were reached at the same experimental conditions for linear orthogonal at  $\pm 45^\circ$  and p–p polarization configurations, respectively. Recording with s–s polarized beams was ineffective since the diffraction efficiency not higher than 1% was reached in this configuration. These results clearly show that the polarization component of the irradiating light parallel to the grating vector is necessary for the effective mass transport. Such polarization dependence, typical to the azobenzene-functionalized polymers, evidences the mechanism of mass transport involving polarization controlled diffusion of azobenzene units in gradient electric field.

The inscribed gratings could be overwritten by subsequent writing. For example, a square structure was generated by successive inscription of two linear gratings with orthogonal grating vectors. AFM image of such structure recorded in the complex C–S is presented in Figure 9. The modulation depths were measured to be 350 and 180 nm for the first and second gratings, respectively. Although recorded at identical conditions the second grating was formed less efficiently resulting in a lower modulation depth. This is different from the polyelectrolyte-based ionic complex materials,<sup>21</sup> where second recording was observed to be even more effective. We suggest some irreversible processes taking place in the investigated materials under irradiation. For a detailed explanation further investigation of the reversibility of the grating recording are in progress.

The thermal stability of the recorded relief structures was studied. It is known that in azobenzene-functionalized polymers the glassy state inherent to polymers and molecular glasses stabilizes both the photoinduced orientation order and the topological structures. However, the SRG formation process is generally less effective in the systems with higher  $T_g$ . In contrast to that we have demonstrated the combination of high recording efficiency with high thermal stability in azobenzene–polyelectrolyte materials.<sup>21,22,28</sup> The network of oppositely charged ions was suggested to be responsible for this effect. The materials under study are also expected to exhibit high thermal stability of SRG due to their ionic nature. It was shown for the material C–S for example. In this experiment the recorded grating was annealed at different temperatures. The erasure of grating was characterized by the total diffraction efficiency normalized to the diffraction efficiency of the grating after recording  $\eta_{\text{norm}} = \eta_r / \eta_{\text{rec}} \cdot 100\%$  in dependence on the temperature. The recorded grating remained stable with  $\eta_{\text{norm}} \approx 90\%$  after heating the sample up to 100  $^\circ\text{C}$ . Heating to 150  $^\circ\text{C}$  erased the grating to  $\eta_{\text{norm}} \approx 75\%$ , but even after heating the sample to 200  $^\circ\text{C}$   $\eta_{\text{norm}} \approx 40\%$  retained. The grating could not be written again onto the thermally treated film that may be explained by further sol–gel condensation, which increases the rigidity of the matrix.

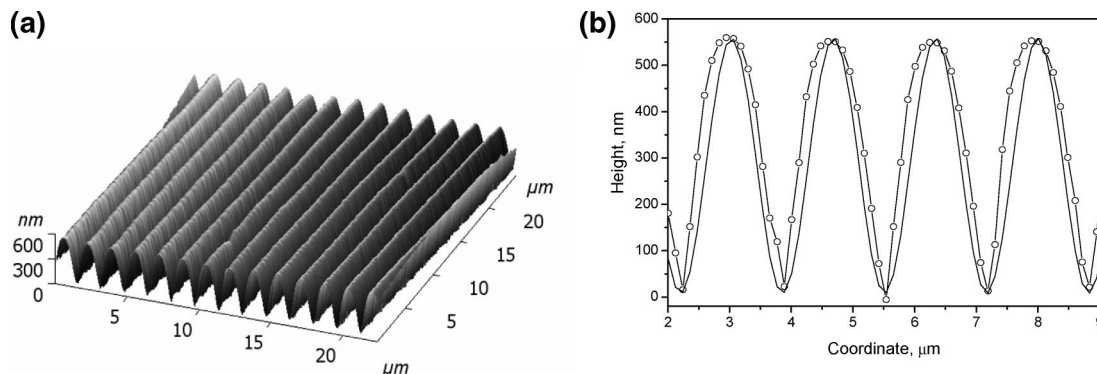


**Figure 6.** AFM image of SRG with modulation depth of 550 nm recorded in the material based on the complex C–S: (a) topology of the grating surface; (b) cross-section of the grating in comparison to the sine function.

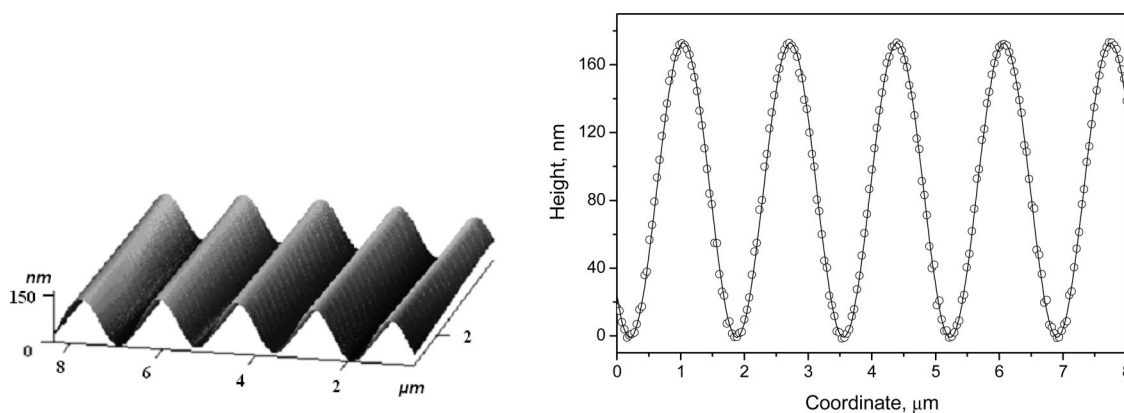


**Figure 7.** AFM image of a shallow grating (modulation depth of 175 nm) recorded in the material based on the complex C–S: (a) topology of the grating surface; (b) cross-section of the grating and the sine function fit to the data.

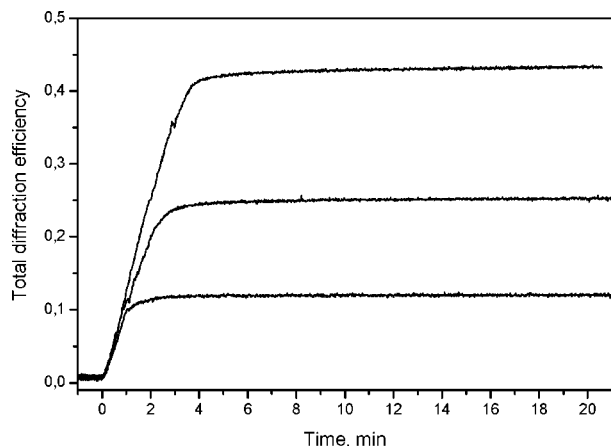


**Figure 8.** Control over grating depth by the irradiation time and stability of the induced gratings. Total diffraction efficiencies of gratings recorded in the material C–S; the recording beams were switched off after 1, 2, and 3 min.

Furthermore the effect of sol–gel condensation on the formation of SRG was investigated. Since sol–gel condensation reactions are supposed to be slow in MeOH, possibly only short polysiloxane oligomers could be formed in this case.<sup>39,40</sup> However, this oligomerization was sufficient for the formation of good optical quality films, and gratings could be readily inscribed immediately after films preparation. Further condensation process could proceed during film storage at room temperature or film heating at 70 °C. The achieved degree of condensation still does not hinder the induction of gratings. Moreover, a slight increase of inscrip-

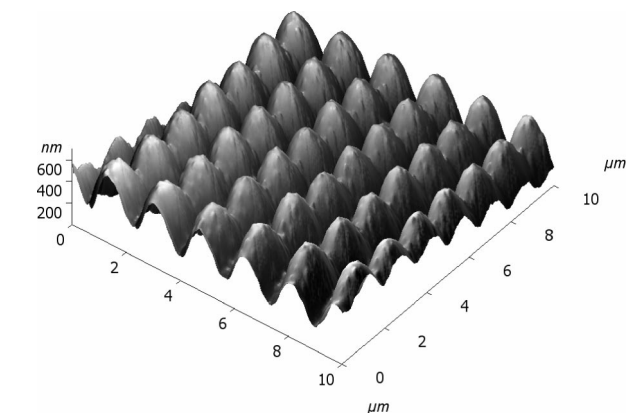


**Figure 9.** AFM image of 2D structure resulting from successive recordings of two linear gratings with orthogonal grating vectors in material C–S.

tion rate was observed. We suppose that the light-induced mass transport is not hindered until certain critical degree of cross linking. For the investigated materials it was reached after the storing films at room temperature for more than a month (films shelf life) or by heating the films at 150 °C for 30 min. The SRG written in the films were stable and were not affected by the time factor.

The effect of cross linking and the role of the material rigidity in the mass transport are worthy of discussing here more in details. In the case of the highly cross-linked sol–gel material one could expect that only local processes such as azobenzene isomerization and orientation take place. The nonlocal process of the translation motion of chromophores

and polymer backbones is impeded by the rigidity of network. For example, the authors<sup>18,31</sup> reported photoinduced birefringence, but the relief gratings could be induced only immediately after the film preparation, while the condensation degree was low enough to have a weakly cross-linked network. However, we suggest here that if the material is not rigid enough the induction of any ordered structures will be counteracted by some relaxation processes resulting in the less effective formation of SRG and their poor stability. This can explain, for instance, the fact that in the azobenzene-functionalized polymers SRG are effectively induced in the glassy state. The latter provides also for the stability of induced SRG at temperatures below the glass transition temperature. We believe that in the sol–gel materials under investigation the effective recording of SRG is provided by the appropriate degree of cross linking. As to molecular mobility the material in the monomer state behaves much as a viscous liquid where any induced order, whether local or wide-ranging, is counteracted by spontaneous diffusion. On the contrary, the strongly cross-linked material behaves as a solid. It allows the induction of local order but restricts translational motion on the scale considerable for SRG. Consequently both these material states are unfavorable for effective light-induced mass transport. There must be an optimum degree of cross linking at which the SRG can be induced most effectively. The results in this study primary prove this suggestion. Further investigations are forthcoming.

#### 4. Conclusions

In summary, we have proposed the supramolecular materials for holographic inscription of surface relief gratings. The

distinctive features of the materials are good film-forming properties, very efficient induction of SRG, in combination with high stability of induced surface relief structures. The materials are based on ionic interaction of azobenzene derivatives with polyelectrolyte matrix formed in situ by the sol–gel reaction. Because of the building-block principle of supramolecular chemistry they are easy to compose from readily available, inexpensive commercial components. Using the ionic interaction to connect photochromic units to the polymer chains allowed very high dye-loading levels without aggregation. What is more, due to this noncovalent bonding the polymer chains got involved in the photoinduced translation motion of azobenzene units resulting in very effective formation of surface relief gratings. For the first time some relaxation processes, which counteract the light-induced formation of surface relief structures were suggested. Under consideration of these processes the influence of network formation and alternatively of glassy state on the efficiency of mass transport and the stability of induced structures was discussed.

**Acknowledgment.** Financial support by the German Federal Ministry of Economics and Technology (InnoNet Project FOTOS) and German Ministry of Education and Research (Project NAMIROs) are gratefully acknowledged. We are grateful to Susanne Kühn for the help with DSC measurements.

**Supporting Information Available:** FTIR spectrum of the material based on dye D and APTES; UV–vis spectrum of the material based on dye D and APTES (PDF file). This material is available free of charge via the Internet at <http://pubs.acs.org>.

CM800106X